Available online at www.sciencedirect.com
SCIENCE DIRECT®
Journal of Sound and Vibration 283 (2005) 1187–1204
JOURNAL OF SOUND AND VIBRATION
www.elsevier.com/locate/jsvi

Short Communication

On the generation of steady motion using fast-vibration

S. Chatterjee*, Saikat Chatterjee, T.K. Singha

Department of Mechanical Engineering, Bengal Engineering College (Deemed University), P.O. Botanic Garden, Howrah 711103, West Bengal, India

Received 14 May 2003; received in revised form 18 November 2003; accepted 21 June 2004
Available online 15 December 2004

1. Introduction

Recent research [1–3] has established that any excitation operating at a time scale much faster compared to the natural time scale of a system may bring forth non-trivial changes in the dynamics of nonlinear systems. In recent literature, such excitations are termed as fast-vibration. Fast-vibration have been shown to effectively change certain characteristics of mechanical systems such as equilibrium states [4], linear stiffness [5], damping [6] and natural frequencies [7]. Suitably designed fast excitation may also significantly influence certain nonlinear features like restoring and energy dissipation characteristics, frequency response and bifurcation behaviour of nonlinear systems. Very elaborate discussions on the numerous applications of fast-vibration in engineering systems may be found in Ref. [8].

In the present article, a very useful application of fast-vibration in producing steady linear motion [8,9] is considered. The fundamental model of such system consists of a rigid slider placed on a friction surface. When the rigid slider is subjected to high frequency tangential and normal excitations bearing a constant phase difference, it moves in one direction with a constant average velocity (with a small high-frequency fluctuation). Thomsen [9] considers an almost similar system, where instead of two phase shifted excitations, the motion is generated due to the asymmetry of co-efficient of friction in forward and backward movement. In this context, one may compare the well-developed theory of ultrasonic motor (USM) [10] with what are considered

*Corresponding author.
E-mail address: shy@mech.becs.ac.in (S. Chatterjee).

0022-460X/$ - see front matter © 2004 Published by Elsevier Ltd.
doi:10.1016/j.jsv.2004.06.042

in Ref. [9] and the present letter. Compared to the traditional USM, the driving principles considered here and also in Ref. [9] are not based on Rayleigh wave propagation.

As the driving force in the system considered here is derived from friction force, it is very much important to model the friction process reliably. A great number of recent phenomenological friction models consider only the macroscopic-degrees-of-freedom. This implies that all microscopic-degrees-of-freedom are much faster than the macroscopic ones. Such an assumption breaks loose when the velocity of sliding becomes comparable to the ratio of microscopic length scale to macroscopic time scale. This microscopic length scale may be of the same order of magnitude as the size of the asperities of the contact surface or the correlation length of the surface roughness. Therefore, when velocity becomes very low, one has to pay attention also in the microscopic-degrees-of-freedom, which are in general faster in dynamics. Moreover, coming to the understanding of the effect of fast vibration, consideration of the interaction of fast microscopic-degrees-of-freedom and the fast excitation becomes important. Few recent models of friction incorporate the microscopic-degrees-of-freedom, and such models are known as dynamic models of friction [11–13]. In the present article, two different types of models of friction, namely Coulomb's dry friction model and LuGre dynamic friction models [11] are considered.

The organisation of the article is as detailed below. In Section 2, two fundamental models consisting of a rigid slider subjected to phase-shifted tangential and normal fast excitation of equal frequencies. In model 1, Coulomb dry friction model is considered, where as in model 2, friction is modelled according to LuGre dynamic friction model. The method of direct partition of motion (MDPM) [8] is used to obtain the steady-state motion of the system. A theoretical analysis is carried out to study the effect of the phase difference between the normal and the tangential excitations as well as the strength of fast excitation on the dynamics of the system. In Section 3, the mathematical model of a practically realisable system is considered. In this system, an embedded high-frequency resonator generates the tangential fast excitation. Though a two-degrees-of-freedom model describes the original system, a simplified single-degree-of-freedom model, equivalent to the model considered in Section 2, is shown to represent a close approximation of the original system. Section 4 discusses some practical aspects of the physical realisation of the theory. Effect of different frequencies in the normal and the tangential directions are also discussed.

2. Fundamental models: rigid slider with phase-shifted tangential and normal fast excitation

2.1. Model 1: Coulomb friction model

The mathematical model of the system consisting of a rigid slider on a frictional surface and subjected to tangential and normal fast excitation is depicted in Fig. 1. The slider is excited by a high-frequency tangential force of amplitude F_T^* and frequency ω and held against a frictional surface by a constant normal load N_0. The amplitude and frequency of fast excitation in the normal direction are ΔN and ω, respectively. The high-frequency component of normal load bears a constant phase shift ϕ with respect to the tangential excitation. Equation of motion of the

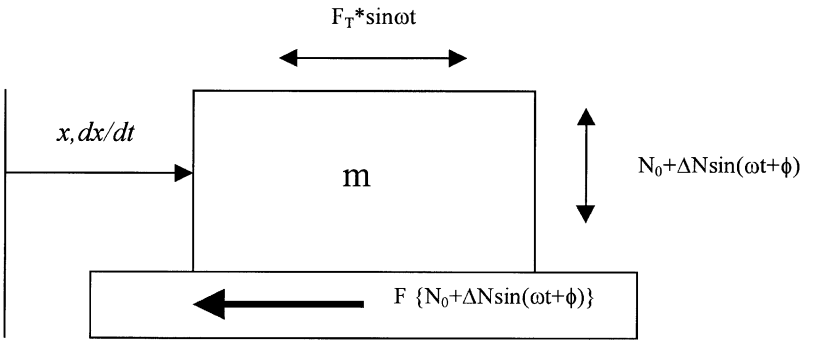

Fig. 1. Mathematical model of the system.

system is given by

$$m\frac{\mathrm{d}^2x}{\mathrm{d}t^2} + F\{N_0 + \Delta N\,\sin(\omega t + \phi)\} = F_T^*\,\sin\,\omega t, \tag{1}$$

where F is friction force per unit normal load and defined as

$$F = \mu\,\mathrm{sgn}\left(\frac{\mathrm{d}x}{\mathrm{d}t}\right),$$

with μ as the coefficient of friction of the frictional surface.

Eq. (1) may be written in the following non-dimensional form:

$$\ddot{X} + \mathrm{Sgn}(\dot{X})\{1 + \alpha\,\sin(\Omega\tau + \phi)\} = F_T\,\sin(\Omega\tau), \tag{2}$$

where

$$X = \frac{x}{x_0}, \quad x_0 = \frac{\mu N_0}{m\omega_0^2}, \quad \alpha = \frac{\Delta N}{N_0}, \quad \Omega = \frac{\omega}{\omega_0}, \quad F_T = \frac{F_T^*}{m\omega_0^2 x_0}.$$

ω_0 is an arbitrary reference frequency and the 'dot' denotes differentiation with respect to the non-dimensional time $\tau = \omega_0 t$.

According to the MDPM [8], when $\Omega \gg 1$ and $F_T\Omega^{-1} \sim O(1)$ or greater, one may split the motion into the slow (Z) and the fast (Ψ) component in the following way:

$$X = Z(\tau) + \Omega^{-1}\Psi(\tau, \Omega\tau), \tag{3}$$

with the assumption that the fast time average of the fast component of the motion is zero, i.e.,

$$\frac{1}{2\pi}\int_0^{2\pi} \Psi(\tau, \Omega\tau)\,\mathrm{d}(\Omega\tau) = 0.$$

Substituting Eq. (3). in Eq. (2), one obtains the following equation governing the slow dynamics of the system:

$$\ddot{Z} + \left(1 - \frac{2}{\pi}\cos^{-1}\left(\frac{\dot{Z}}{q}\right) - \frac{2\alpha}{\pi}\sin\left(\cos^{-1}\left(\frac{\dot{Z}}{q}\right)\right)\sin(\phi)\right) = 0, \tag{4}$$

where

$$q = \Omega^{-1} F_T$$

Eq. (4) describes the dynamics of the system in the natural time scale (fast time scale) of the system. From Eq. (4), one observes that at steady state the slider moves with a constant average velocity V that may be obtained by solving the following nonlinear algebraic equation:

$$1 - \frac{2}{\pi}\cos^{-1}\left(\frac{V}{q}\right) - \frac{2\alpha}{\pi}\sin\left(\cos^{-1}\left(\frac{V}{q}\right)\right)\sin(\phi) = 0. \tag{5}$$

When velocity is small, i.e., $\mathrm{d}Z/\mathrm{d}\tau \ll q$, one obtains a linear equation describing the slow dynamics as

$$\ddot{Z} + \frac{2\dot{Z}}{\pi q} = \frac{2}{\pi}\,\alpha\,\sin(\phi). \tag{6}$$

Under such circumstances, the average steady-state sliding velocity V of the slider is obtained as

$$V = q\alpha\,\sin(\phi). \tag{7}$$

2.2. Model 2: LuGre friction model

When LuGre friction model is considered, the equation of motion of the system depicted in Fig. 1 is given by

$$\begin{aligned} &m\,\frac{\mathrm{d}^2x}{\mathrm{d}t^2} + (N_0 + \Delta N\,\sin(\omega t + \phi))F = F_T^*\,\sin\,\omega t,\\ &F = \sigma_0^* z + \sigma_1^*\,\frac{\mathrm{d}z}{\mathrm{d}t},\\ &\frac{\mathrm{d}z}{\mathrm{d}t} = \frac{\mathrm{d}x}{\mathrm{d}t} - \frac{\sigma_0^* z}{\mu}\left|\frac{\mathrm{d}x}{\mathrm{d}t}\right|, \end{aligned} \tag{8}$$

where F is friction force due to unit normal load, and σ_0^* and σ_1^* are LuGre model parameters. The variable z is a state variable as described in the LuGre model, which considers that any frictional interface is made of elastic spring like bristles [11,12]. Physically, z describes the average deflection of the interface bristles.

Eq. (8) may be written in the following non-dimensional form:

$$\begin{aligned} &\ddot{X} + (1 + \alpha\,\sin(\Omega\tau + \phi))\left(\sigma_0 Z_b + \sigma_1\dot{X} - \frac{\sigma_1\sigma_0 Z_b}{\mu}\,|\dot{X}|\right) = F_T\,\sin(\Omega\tau),\\ &\frac{\mathrm{d}Z_b}{\mathrm{d}\tau} = \dot{X} - \frac{\sigma_0|\dot{X}|}{\mu}\,Z_b, \end{aligned} \tag{9}$$

where the non-dimensional terms are as defined below:

$$X = \frac{x}{x_0}, \quad Z_b = \frac{z}{x_0}, \quad \sigma_0 = \frac{N_0\sigma_0^*}{m\omega_0^2}, \quad \sigma_1 = \frac{N_0\sigma_1^*}{m\omega_0}, \quad x_0 = \frac{N_0}{m\omega_0^2}$$

and ω_0 is an arbitrary reference frequency.

According to the MDPM [8], one may split X and Z_b into slow (subscripts s) and fast components (subscripts f) as follows:

$$X = X_s(\tau) + \Omega^{-1} X_f(\tau, \Omega\tau),$$
$$Z_b = Z_s(\tau) + \Omega^{-1} Z_f(\tau, \Omega\tau), \tag{10}$$

with the assumptions that the fast time averages of the fast components of motion are zero, i.e.,

$$\frac{1}{2\pi}\int_0^{2\pi} X_f(\tau, \Omega\tau)\,\mathrm{d}(\Omega\tau) = 0$$

and

$$\frac{1}{2\pi}\int_0^{2\pi} Z_f(\tau, \Omega\tau)\,\mathrm{d}(\Omega\tau) = 0.$$

Substituting Eq. (10) in Eq. (9), one obtains

$$\ddot{X}_s + \frac{1}{2\pi}\int_0^{2\pi} \Im(\theta)\,\mathrm{d}\theta = 0,$$
$$\dot{Z}_s = \dot{X}_s - \frac{1}{2\pi}\int_0^{2\pi} \Re(\theta)\,\mathrm{d}\theta, \tag{11}$$

where

$$\Im(\theta) = (1 + \alpha\,\sin(\theta + \phi))\left(\sigma_0 Z_s + \sigma_1(\dot{X}_s - q\,\cos\,\theta) - \frac{\sigma_1\sigma_0 Z_s}{\mu}\,|\dot{X}_s - q\,\cos\,\theta|\right)$$

and

$$\Re(\theta) = \frac{\sigma_0|\dot{X}_s - q\,\cos\,\theta|}{\mu}\,Z_s.$$

After computing the above integrals, one finally obtains the following equation:

$$\ddot{X}_s + \sigma_0 Z_s + \sigma_1 \dot{X}_s - \frac{\sigma_1 q\alpha}{2}\,\sin\,\phi - \frac{\sigma_1\sigma_0}{\mu}\,Z_s(f_1(\dot{X}_s) + f_2(\dot{X}_s)) = 0,$$
$$\dot{Z}_s = \dot{X}_s - \frac{\sigma_0}{\mu}\,Z_s f_1(\dot{X}_s), \tag{12}$$

where

$$f_1(\dot{X}_s) = \frac{1}{\pi}\{\dot{X}_s(\pi - 2\theta_1) + 2q\,\sin\,\theta_1\},$$

$$f_2(\dot{X}_s) = \frac{\alpha\,\sin\,\phi}{2\pi}\,\{q\,\sin\,2\theta_1 - 4\dot{X}_s\,\sin\,\theta_1 - q(\pi - 2\theta_1)\},$$

$$\theta_1 = \cos^{-1}\left(\frac{\dot{X}_s}{q}\right).$$

Now substituting

$$Y = \sigma_0 Z_s$$

and

$$\varepsilon = \frac{1}{\sigma_0}$$

in Eq. (12) one obtains

$$\ddot{X}_s + Y + \sigma_1 \dot{X}_s - \frac{\sigma_1 q\alpha}{2} \sin\phi - \frac{\sigma_1}{\mu} Y(f_1(\dot{X}_s) + f_2(\dot{X}_s)) = 0,$$

$$\varepsilon \dot{Y} = \dot{X}_s - \frac{Y}{\mu} f_1(\dot{X}_s). \tag{13}$$

As σ_0 is generally a large quantity, $\varepsilon \ll 1$ and one may find that Eq. (13) is in standard singular perturbation form. Thus, the slow manifold of the system is described by

$$Y = \frac{\mu \dot{X}_s}{f_1(\dot{X}_s)}. \tag{14}$$

After enabling the following coordinate and time transformation [14]:

$$Y^* = Y - \frac{\mu \dot{X}_s}{f_1(\dot{X}_s)},$$

$$\tau^* = \frac{\tau}{\varepsilon}$$

and treating velocity as constant, one obtains the boundary layer equation as

$$\frac{\mathrm{d}Y^*}{\mathrm{d}\tau^*} = -\frac{Y^* f_1(\dot{X}_s)}{\mu}. \tag{15}$$

The trivial equilibrium of the boundary layer equation is uniformly asymptotically stable for all velocities. Therefore, according to Tikhonov theorem [15] the slow manifold describes the reduced-order model of the system accurate to ε order. Thus, the slow dynamics of the system is given by

$$\ddot{X}_s + \dot{X}_s \left\{ \frac{\mu}{f_1} - \frac{\sigma_1 f_2}{f_1} \right\} - \frac{\sigma_1 q\alpha}{2} \sin\phi = 0. \tag{16}$$

Finally, one obtains the steady-state average constant velocity of sliding (V) by solving the following equation:

$$V \left\{ \frac{\mu}{f_1} - \frac{\sigma_1 f_2}{f_1} \right\} - \frac{\sigma_1 q\alpha}{2} \sin\phi = 0. \tag{17}$$

For small velocity $V \ll q$, one obtains the linearised dynamics as described by

$$\ddot{X}_s + \tfrac{\pi\mu}{2q} \dot{X}_s - \tfrac{1}{2}\sigma_1 q\alpha \sin\phi = 0. \tag{18}$$

Thus, for small velocity $V \ll q$, one obtains

$$V = \frac{\sigma_1 \alpha q^2 \sin \phi}{\pi \mu}. \tag{19}$$

2.3. Results and discussion: effect of parameters

It has already been mentioned that due to the simultaneous normal and tangential high-frequency excitations, the slider moves with a constant average velocity. In support of the above statement, direct numerical simulation of equation of motion (2) and (9) are carried out in MATLAB SIMULINK using "Dormand-Prince 8(5,3)" algorithm and the simulated displacement time histories are depicted in Fig. 2. From Fig. 2, one may have already noticed that a high-frequency component is always present in the time history. The amplitude of this high-frequency component depends on the frequency of tangential excitation. The amplitude of high-frequency component in the system response decreases with the increasing excitation frequency. However, for significant effect of fast vibration one should keep the strength of the excitation q $(= F_T \Omega^{-1}) \sim O(1)$. In what follows, the effect of different input parameters on the steady-state motion of the system is discussed.

2.3.1. Model 1

So far as the steady-state average velocity of the slider is concerned, it is apparent from Eqs. (5) and (7) that the strength of the excitations q $(= F_T \Omega^{-1})$ and α are the important parameters along with the phase difference ϕ between the normal and tangential excitations. From Eqs. (5) and (7), one infers that the highest average velocity V is obtained when the excitations are in quadrature. Results obtained by solving Eq. (5) are plotted in Fig. 3 depicting the variation of V with ϕ, q and

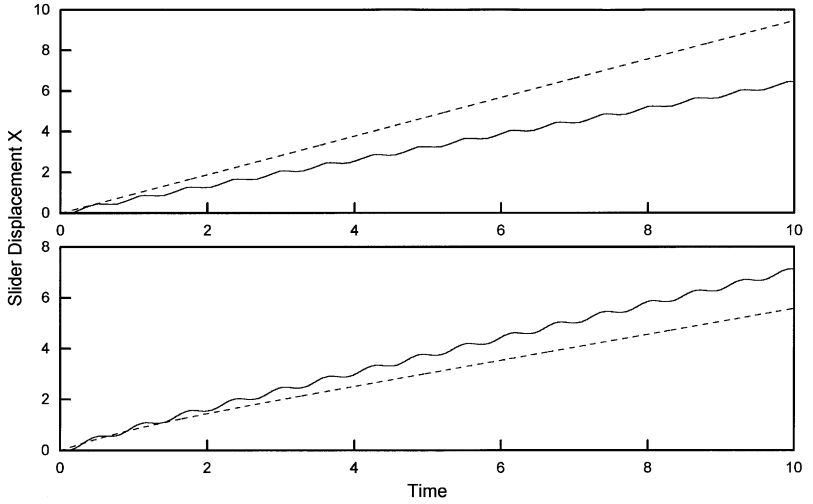

Fig. 2. Displacement time history of the slider. $\alpha = 1$, $\phi = \pi/2$. —, $F_T = 10, \Omega = 10$; - - - -, $F_T = 1000$, $\Omega = 1000$: (a) Coulomb friction model; (b) LuGre friction model, $\sigma_0 = 100$, $\sigma_1 = 1$, $\mu = 0.4$.

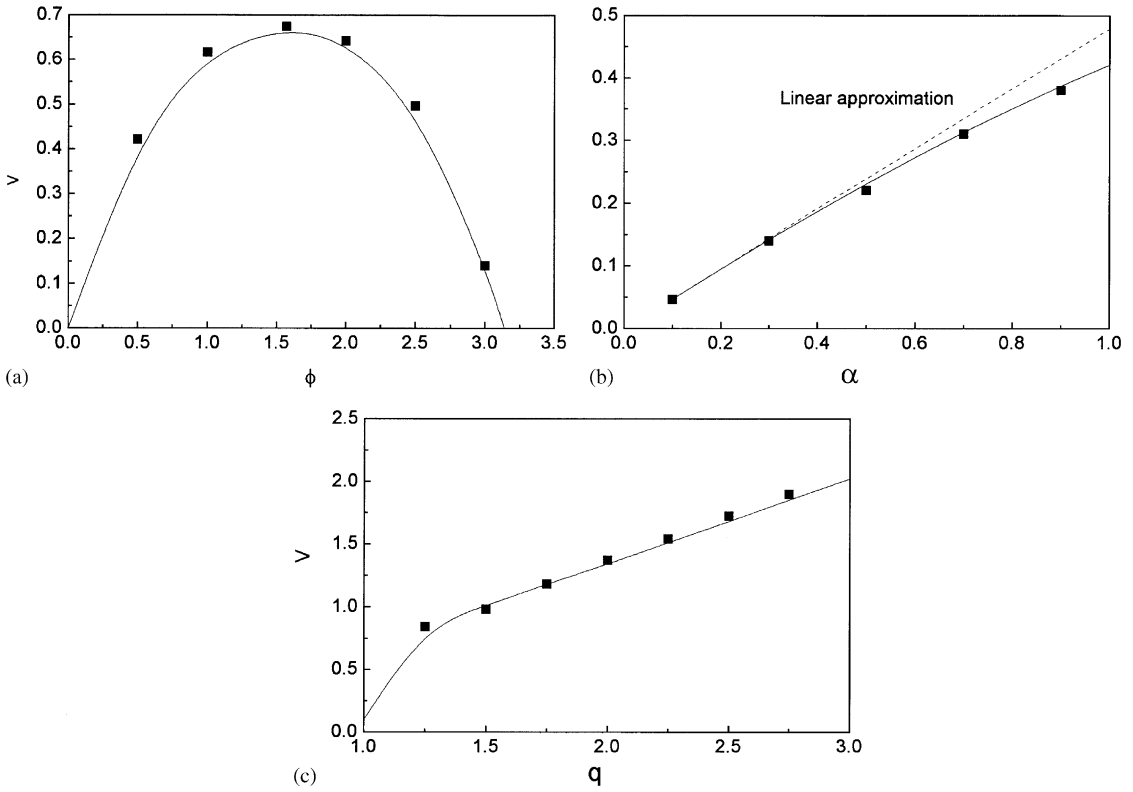

Fig. 3. Variation of average sliding velocity with different parameters. —, analytical; ■, numerical simulation: (a) $\alpha = 1,\ q = 1$; (b) $\phi = 0.5,\ q = 1$; (c) $\phi = 1.57,\ \alpha = 1$.

α. These results are also compared with that obtained from the direct numerical simulation of equation motion (2). From Fig. 3, one infers that in general the average sliding velocity increases with the strength parameters α and q. One should also note that Fig. 3(a) is plotted for the values of ϕ ranging between 0 and π, for which the sliding velocity V is positive. For values of ϕ between $-\pi$ and 0, one obtains negative velocity of sliding. One may observe from Eq. (7) that for some parameter values (particularly for small q and α), the average velocity V is linearly proportional to the strength parameters q and α.

It may be mentioned here that the equations and expressions obtained hitherto in the section are for no-load condition, i.e. when no external load tends to impede the motion of the system. Under the action of an impeding external load (say constant) one obtains the load speed curve depicted in Fig. 4(a) by solving the following equation:

$$1 - \frac{2}{\pi}\cos^{-1}\left(\frac{V}{q}\right) - \frac{2\alpha}{\pi}\sin\left(\cos^{-1}\left(\frac{V}{q}\right)\right)\sin(\phi) + L = 0, \tag{20}$$

where L is the non-dimensional load and the non-dimensionalisation is done with respect to $mx_0\omega^2$. From Eq. (20), one obtains the following expression for the "blocking force" (the amount

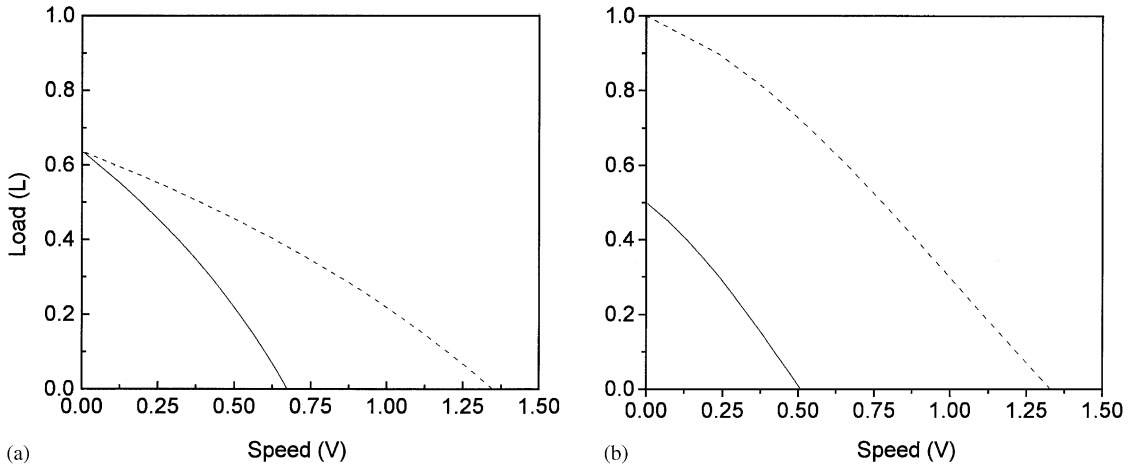

Fig. 4. Speed-load characteristics of the slider. $\alpha = 1,\ \phi = \pi/2$. —, $q = 1$; - - - - $q = 2$: (a) Coulomb model; (b) LuGre model, $\sigma_1 = 1,\ \mu = 0.4$.

of external tangential load to cause the complete seizure of the motion) L_b:

$$L_b = \frac{2\alpha}{\pi} \sin \phi. \tag{21}$$

In the original dimensional form, "blocking-force" may be expressed as

$$\text{Dimensional blocking force} = \frac{2}{\pi} \mu \Delta N \sin \phi. \tag{22}$$

2.3.2. Model 2

For the LuGre model of friction, the variation of V with ϕ, α, μ, and q are obtained by solving Eq. (17) and depicted in Fig. 5. From Fig. 5, one observes that the highest velocity of sliding is possible for $\phi = \pi/2$. The velocity V increases with the strength of the excitations α and q, and decreases with increasing value of μ. Such relationships are also obtained from the approximate linearised equation (19) (valid for only small values of q and α).

In case of the LuGre friction model, the speed-load characteristics of the system is obtained by solving the following equation:

$$V\left\{\frac{\mu}{f_1} - \frac{\sigma_1 f_2}{f_1}\right\} - \frac{\sigma_1 q \alpha}{2} \sin \phi + L = 0. \tag{23}$$

Typical speed load characteristics of the slider for the LuGre friction model are depicted in Fig. 4(b).

The non-dimensional "blocking force" is obtained as

$$L_b = \frac{\sigma_1 q \alpha}{2} \sin \phi. \tag{24}$$

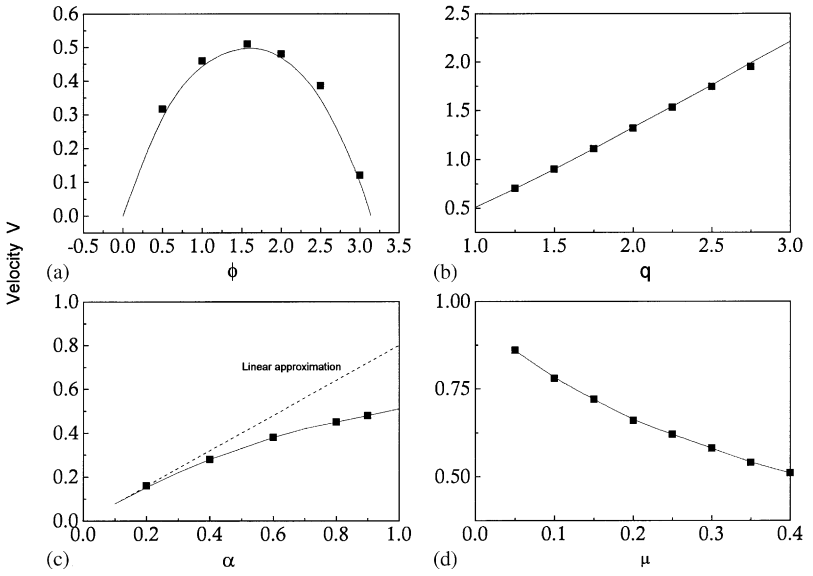

Fig. 5. Variation of average sliding speed with system parameters in case of LuGre model of friction. —, analytical; ■, numerical simulation ($\sigma_0 = 100$): (a) $\sigma_1 = 1,\ \mu = 0.4,\ \alpha = 1,\ q = 1$; (b) $\sigma_1 = 1,\ \mu = 0.4,\ \alpha = 1,\ \phi = 1.57$; (c) $\sigma_1 = 1,\ \mu = 0.4,\ q = 1,\ \phi = 1.57$; (d) $\sigma_1 = 1,\ \alpha = 1,\ q = 1,\ \phi = 1.57$.

In terms of the dimensional parameters, expression for "blocking force" becomes

$$\text{Blocking force} = \frac{1}{2}\frac{\sigma_1^*}{m}\frac{F_T^*}{\omega}\Delta N \sin\phi. \tag{25}$$

From Eq. (25), one may note that in case of the LuGre model, "blocking force" depends on the tangential excitation as well as the inertia of the slider. This is in contrast with the case of model 1, where the blocking force (Eq. (22)) does not depend on the tangential excitation parameters or mass of the slider. The dependence of the blocking force on the mass of the slider seems to be somewhat unrealistic. However, such dependence is removed if the LuGre model parameter σ_1^* is proportional to the mass of the slider. Moreover, it is interesting to note that unlike in the case of model 1, blocking force does not show any dependence on co-efficient of friction when LuGre friction model is considered.

3. Model of a practically realisable system

In the fundamental model considered in the previous section, the rigid slider is subjected to fast-excitations in the tangential and the normal directions. Though it is possible to generate the normal excitation (along with a pre-load) using a piezoelectric actuator, particularly when the slider moves along a guide-way without any clearances, generation of the tangential excitation is involved. One possible solution of generating the tangential excitation may be using an embedded resonator, which is realised by a mechanical resonator clamped at one end inside the slider and

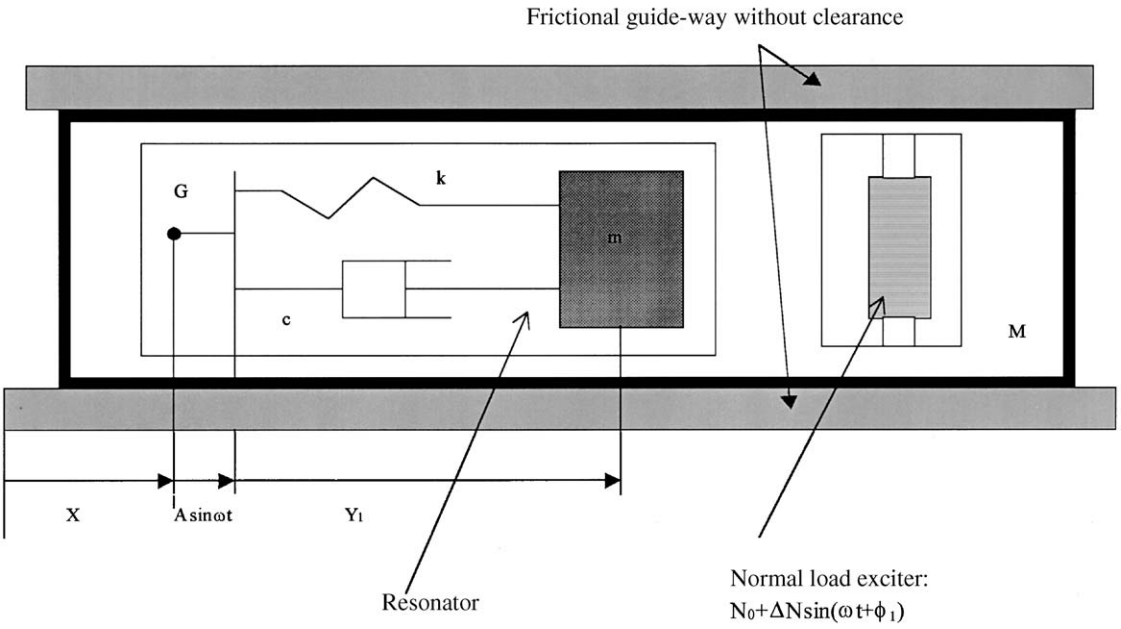

Fig. 6. Mathematical model of a practically realisable system.

driven near high-frequency resonance by a piezo exciter. The present section considers such a practically realisable system depicted in Fig. 6. The mathematical model of the original system may be represented by a two-degrees-of-freedom system. However, it is shown that an approximate single-degree-of-freedom model, equivalent to what has been considered in Section 2, suffices for some practical purposes.

3.1. Mathematical model and equation of motion

The equation of motion of the system depicted in Fig. 6 may be written as

$$(M+m)\frac{\mathrm{d}^2X}{\mathrm{d}t^2}+2\mu(N_0+\Delta N\,\sin(\omega t+\phi_1))\mathrm{sgn}\left(\frac{\mathrm{d}X}{\mathrm{d}t}\right)+m\left(\frac{\mathrm{d}^2Y_1}{\mathrm{d}t^2}-A\omega^2\,\sin\,\omega t\right)=0, \tag{26}$$

$$m\frac{\mathrm{d}^2Y_1}{\mathrm{d}t^2}+c\frac{\mathrm{d}Y_1}{\mathrm{d}t}+kY_1+m\frac{\mathrm{d}^2X}{\mathrm{d}t^2}=mA\omega^2\,\sin\,\omega t. \tag{27}$$

One obtains the following non-dimensional form of equation of motion:

$$\ddot{x}+\mathrm{sgn}(\dot{x})\{1+\alpha\,\sin(\Omega\tau+\phi_1)\}+r_m\{\ddot{y}_1-a\Omega^2\,\sin\,\Omega\tau\}=0, \tag{28}$$

$$\ddot{y}_1+2\xi\Omega_n\dot{y}_1+\Omega_n^2y_1+\ddot{x}=a\Omega^2\,\sin\,\Omega\tau, \tag{29}$$

where the non-dimensional quantities are as defined below:

$$x = \frac{X}{x_0}, \quad y_1 = \frac{Y_1}{x_0}, \quad \Omega_n = \frac{1}{\omega_0}\sqrt{\frac{k}{m}}, \quad r_m = \frac{m}{m+M},$$

$$a = \frac{A}{x_0}, \quad \Omega = \frac{\omega}{\omega_0}, \quad x_0 = \frac{2\mu N_0}{(m+M)\omega_0^2}, \quad \alpha = \frac{\Delta N}{N_0}, \quad \tau = \omega_0 t.$$

3.2. Single-degree-of-freedom approximation

From Eq. (28), one may note that the second term of the LHS is significantly small compared to the other terms (as $\alpha < 1$ and $\Omega \gg 1$). Thus substituting

$$\ddot{x} = -r_m\{\ddot{y}_1 - a\Omega^2 \sin \Omega\tau\} \tag{30}$$

in Eq. (29), one obtains

$$(1 - r_m)\ddot{y}_1 + 2\xi\Omega_n\dot{y}_1 + \Omega_n^2 y_1 = (1 - r_m)a\Omega^2 \sin \Omega\tau. \tag{31}$$

The steady-state solution of Eq. (31) is obtained as

$$y_1 = Y_0 \sin(\Omega\tau - \theta), \tag{32}$$

where

$$Y_0 = \frac{(1 - r_m)a\Omega^2}{\sqrt{(\Omega_n^2 - \Omega^2(1 - r_m))^2 + (2\xi\Omega_n\Omega)^2}}, \quad \tan\theta = \frac{2\xi\Omega_n\Omega}{\Omega_n^2 - \Omega^2(1 - r_m)}.$$

Using Eq. (32) in Eq. (28), one obtains

$$\ddot{x} + \mathrm{sgn}(\dot{x})\{1 + \alpha \sin(\Omega\tau + \phi_1)\} = F_T \sin(\Omega\tau - \theta_1), \tag{33}$$

where

$$F_T = r_m\Omega^2\sqrt{(Y_0 \cos\theta + a)^2 + (Y_0 \sin\theta)^2},$$

$$\tan\theta_1 = \frac{Y_0 \sin\theta}{Y_0 \cos\theta + a}.$$

Using the following time translation:

$$\Omega\tau - \theta_1 = \Omega\tau^*,$$

one transforms Eq. (33) into

$$\frac{\mathrm{d}^2x}{\mathrm{d}\tau^{*2}} + \mathrm{sgn}\left(\frac{\mathrm{d}x}{\mathrm{d}\tau^*}\right)\{1 + \alpha \sin(\Omega\tau^* + \phi)\} = F_T \sin \Omega\tau^*, \tag{34}$$

where

$$\phi = \phi_1 + \theta_1.$$

Eq. (34) is an approximate single-degree-of-freedom model of the system. In order to validate the approximation, Eqs. (28), (29) and (34) are numerically simulated. The results of numerical

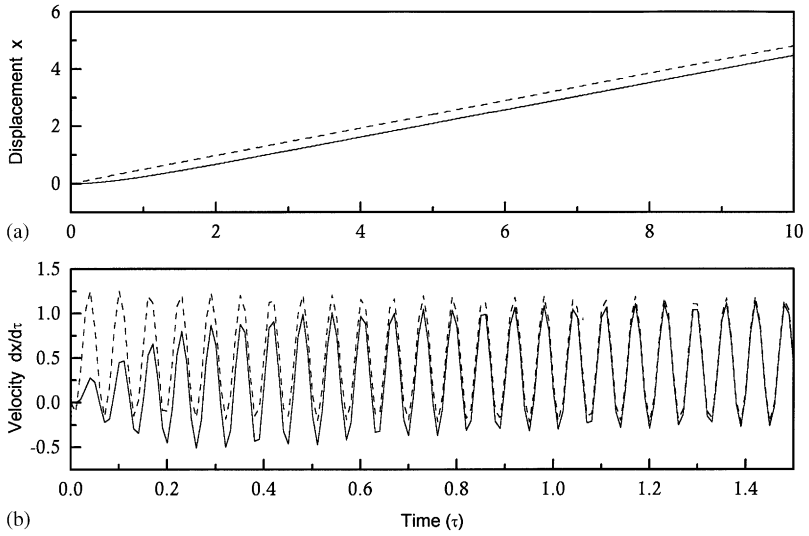

Fig. 7. (a,b) Displacement and velocity time history of the slider with embedded resonator. —, two-degree-of-freedom model, - - -, single-degree-of-freedom model. $r_m = 0.1,\ \Omega_n = \Omega = 100,\ a = 0.01,\ \alpha = 1,\ \phi_1 = 0.85,\ \xi = 0.05$.

simulation are plotted in Fig. 7 to compare the velocity and displacement time histories of the full and the approximate systems. From Fig. 7, one observes little difference in the steady-state velocity time histories between the full and the approximate models. However, there exists a constant steady state difference between the displacement characteristics.

One may note that the approximate single-degree-of-freedom model (34) of the system is equivalent to the fundamental model given by Eq. (2). It is also possible to establish the similar equivalence for LuGre friction model as well. Therefore, it is reasonable to consider the fundamental models for the quantitative and qualitative estimation of the steady-state velocity characteristics of the system. However, for studying displacement characteristics, one requires a complete model of the system.

4. A physical example and discussions

In this section an example system is considered for discussing some important practical aspects of the physical implementation of the theory. The example system is similar to what has been shown in Fig. 6. The frictional load due to the weight of the slider is neglected as this frictional load may be reduced to a very low value by transferring the weight of the slider through rolling friction contact. The parameter values of the system considered are listed in Table 1.

Selection of the frequency of excitations and the amplitude of the base excitation given to the horizontal resonator is very important. As mentioned in Section 2.3, for smooth oscillation free movement of the slider it is required that $q\ (= \Omega^{-1}F_T) \sim O(1)$, and the frequency should be high enough to keep the amplitude (non-dimensional value $\sim q\Omega^{-1}$) of the high-frequency (Ω) vibration of the slider below the acceptable limit. In order to produce substantial horizontal force,

Table 1

Mass of the slider M	1 kg
Mass of the oscillator m	0.1 kg
Natural frequency of the oscillator $(k/m)^{1/2}$	3500 rad/s
Damping factor of the oscillator $0.5c/(km)^{1/2}$	0.05
Normal preload N_0	1.0 N
Amplitude of normal load variation ΔN	1.0 N
Amplitude of base excitation given to the oscillator A	100 μm
Frequency of fast excitation ω	3500 rad/s
Phase ϕ_1	0
Coefficient of friction μ	0.1

$\omega_0 = 1$ rad/s.

excitation frequency in the tangential direction is tuned to the natural frequency of the oscillator. However, while choosing the excitation frequency, one should also keep in mind that very high-frequency tangential excitation gives rise to very strong horizontal excitation, and that the system should be capable of withstanding that load.

With the parameter values assumed above, the system (according to the theory described here) is equivalent to the fundamental system shown in Fig. 1, where a rigid slider of mass 1.1 kg is driven by the tangential and the normal excitations of magnitude $910.95 \sin(3500t)$ and $1 + \sin(3500t + 0.733)$ Newton, respectively. Here one may check that the non-dimensional quantity $q = \Omega^{-1} F_T$ (strength of tangential fast excitation) is 1.301, which satisfies the requirement that $q \sim O(1)$. Thus, solving Eq. (5) one finds the average velocity of sliding as 0.12 m/s, and this is also verified by numerically simulating Eqs. (26) and (27). The amplitude of high-frequency oscillation is 67.6 μm in the present example. If the amplitude of high-frequency oscillation in the present example is not acceptable, it can be reduced to a lower value by driving a high-frequency resonator with a base excitation of lower amplitude and higher frequency. For example, the amplitude of high-frequency oscillation can be reduced to 6.76 μm by driving a 5570.42 Hz resonator by a base excitation of amplitude 10 μm and frequency 35000 rad/s. In doing so, one of course keep q and ϕ, and hence the sliding velocity same. However, this reduction in the amplitude of high-frequency oscillation is obtained only at the cost of stronger horizontal force of excitation (which is now increased to 9109.5 N).

It may be mentioned here that the hardware realisation of the model discussed above is not very difficult. The normal force excitation may be generated by a piezoelectric actuator, which produces 1 N preload along with a variable load of amplitude 1 N and frequency 557 Hz. The tangential excitation is produced by driving the base of a resonator (with the natural frequency 557 Hz and damping factor 0.05) by a piezoelectric exciter (fixed to the slider) at 557 Hz frequency and amplitude 0.1 mm. If both the actuator and the exciter are driven by the same signal source, it may be possible to maintain the same frequency and a constant phase shift between the two signal channels. Of course, maintaining the same frequency in the normal and tangential directions is very important for producing the steady sliding of the slider. In case of a very small difference between the tangential and normal excitation frequencies, instead of unidirectional steady sliding,

low-frequency oscillations of the slider takes place around an equilibrium (may be shifted from the initial position).

However, when it is not possible to synchronize the excitations at equal frequencies, the slider can still move with a constant velocity if the tangential and the normal excitation frequencies are substantially different and the phase difference is proper. It may be noted here that the present theoretical formalism cannot accommodate the situation when the fast vibration frequencies in the two directions are different, because such a condition involves more than two disparate time scales. Under such circumstances, a more general theoretical setup incorporating multiple time scales is required. Development of such a methodology is beyond the scope of the present letter. It may also be mentioned here that the reduction of the two-degrees-of-freedom model to an approximate single-degree-of-freedom model is not valid for totally different frequencies of the tangential and the normal excitations. However, remaining in the present theoretical setup, one can analyse the qualitative effect of very slight difference in the frequencies of excitations (see Appendix A).

Effect of using different frequencies in the normal and the tangential excitations is studied by numerically simulating Eqs. (28) and (29) with the non-dimensional parameter values calculated from the values given in Table 1. The difference of excitation frequencies in the normal and the

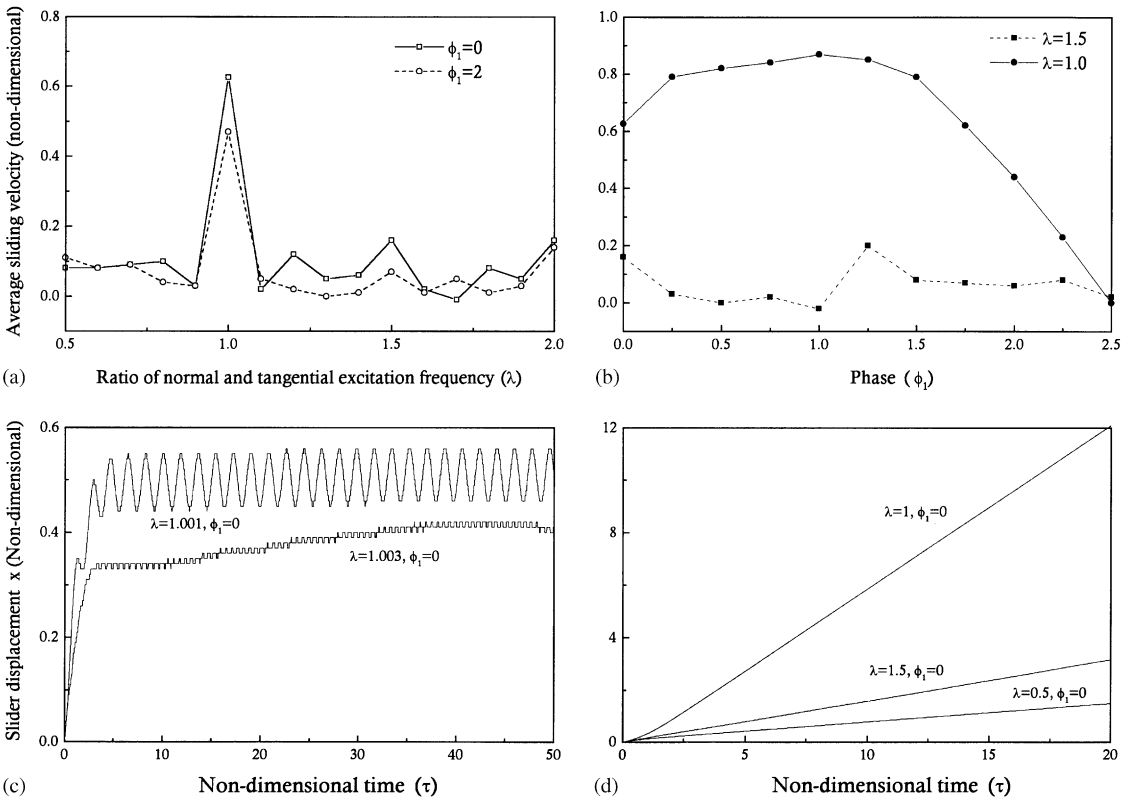

Fig. 8. Effect of different frequencies of normal and tangential excitations on the dynamics of sliding. $\Omega = \Omega_n = 3500$, $a = 0.00055$, $\mu = 0.1$, $r_m = 0.09$, $\alpha = 1$.

tangential directions are modelled by introducing a parameter λ, which is defined as the ratio of the normal and the tangential excitation frequencies. Results of numerical simulations for different parameter values are shown in Fig. 8. Figs. 8(a) and (b) depict the variation of the average steady-state sliding velocity with λ and ϕ_1, respectively. From these figures, one may observe that equal frequencies in both the directions ($\lambda = 1$) produce the strongest effect both in terms of sliding velocity as well as load-carrying capacity [i.e. blocking force] (results are not shown). Though steady sliding is still possible for different frequencies in the normal and the tangential directions, corresponding velocities of sliding (see Fig. 8(d) for displacement time histories of the slider) and the load carrying capacities are substantially weaker as compared to that are obtainable for equal frequencies. However, as shown in Fig. 8(c), a very small difference in the excitation frequencies results in low-frequency oscillation of the slider instead of steady unidirectional motion. The frequency of this oscillation is exactly equal to the frequency difference, and the amplitude of the oscillation decreases with the increasing amount of frequency detuning.

5. Conclusions

A rigid slider moves with a constant velocity on a friction surface when simultaneously excited by high-frequency tangential and normal excitations bearing a constant phase difference. Two different fundamental models are considered in the present article for studying such effect. Two different models of friction, namely, the Coulomb dry friction model and the LuGre dynamic friction models are considered to study the effect of different parameters on the velocity of sliding. It is shown that the maximum possible velocity of sliding is achieved when the excitations are in quadrature.

A two-degrees-of-freedom model of a practically realisable system consisting of an embedded resonator for generating the tangential excitation is also considered. It is shown that so far as the prediction of the steady-state sliding velocity is concerned, an approximate single-degree-of-freedom model of the system suffices to a great extent and more importantly, this approximate model is equivalent to the fundamental model described earlier.

Finally, an example system is considered to discuss the physical implementation of the theory. The effect of using different frequencies in the normal and tangential excitations is also discussed. It is observed that though steady sliding may be produced by two substantially different frequencies of excitation, the corresponding sliding is not strong enough (both in terms of velocity of sliding and load carrying capacity) as compared to that can be produced by synchronous frequencies of excitations. However, when equal frequencies are used in both the directions, one should be careful enough not to allow even a very slight difference in the frequencies, because that, instead of steady sliding, may give rise to low-frequency oscillation of the slider.

Appendix A

In the main text of the present letter it has been shown that when the excitation frequencies in the normal and the tangential directions are only slightly different, the slider either sticks or

oscillates around an equilibrium position. A theoretical explanation of the phenomenon is given here. As it has been shown in Section 3 that an original two-degrees-of-freedom model can be effectively reduced to an equivalent single-degree-of-freedom model, the present discussion starts with the fundamental model described by Eq. (2). When a very small difference of the excitation frequencies in the normal and the tangential directions are allowed, Eq. (2) may be rewritten as

$$\ddot{X} + \mathrm{Sgn}(\dot{X})\{1 + \alpha \sin(\Omega\tau + \Delta\Omega\tau + \phi)\} = F_T \sin(\Omega\tau),$$

or

$$\ddot{X} + \mathrm{Sgn}(\dot{X})\{1 + \alpha \sin(\Omega\tau + \psi(\tau))\} = F_T \sin(\Omega\tau), \tag{A.1}$$

where

$$\psi(\tau) = \Delta\Omega\tau + \phi,$$

and $\Delta\Omega$ is the small difference in the normal and the tangential excitation frequencies. Thus under such circumstances, one may consider that the phase difference between the normal and the tangential excitations is a slowly varying function of time ($\psi(\tau)$). Using the similar procedure as described in Section 2, one finally represents the slow dynamics of the system as

$$\ddot{Z} + \left(1 - \frac{2}{\pi}\cos^{-1}\left(\frac{\dot{Z}}{q}\right) - \frac{2\alpha}{\pi}\sin\left(\cos^{-1}\left(\frac{\dot{Z}}{q}\right)\right)\sin(\psi(\tau))\right) = 0. \tag{A.2}$$

Eq. (A.2) is nonlinear and can be numerically simulated to study the slow dynamics of the slider. Eq. (A.2) suggests that steady unidirectional sliding is not possible when the excitation frequencies are only slightly different. To investigate further into the qualitative nature of the motion, Eq. (A.2) is linearised (which is valid at least for small values of α) to yield

$$\ddot{Z} + \frac{2}{\pi}\left(\frac{\dot{Z}}{q}\right) = \frac{2\alpha}{\pi}\sin(\Delta\Omega\tau + \phi). \tag{A.3}$$

From Eq. (A.3), one may conclude that the slider oscillates at low frequency ($\Delta\Omega$).

References

[1] I.I. Blekhman, Forming properties of nonlinear mechanical systems by means of vibration, *Proceedings of IUTAM/IFToMM Symposium in Synthesis of Nonlinear Dynamical Systems*, Riga, Latvia, 24–25 August, 1998, pp. 1–11.

[2] A. Fidlin, J.J. Thomsen, Predicting vibration-induced displacement for a resonant friction slider, *European Journal of Mechanics of Solids* 20 (2001) 155–166.

[3] J.J. Thomsen, Some general effects of strong high-frequency excitation: stiffening, biasing, and smoothening, *Journal of Sound and Vibration* 253 (4) (2002) 807–831.

[4] J.J. Thomsen, D.M. Tcherniak, Chelomei's pendulum explained, *Proceedings of Royal Society of London* 457 (2001) 1889–1913.

[5] J.S. Jensen, D.M. Tcherniak, J.J. Thomsen, Stiffening effects of high frequency excitation: experiments for an axially loaded beam, *Journal of Applied Mechanics* 67 (2) (2000) 397–402.

[6] S. Chatterjee, T.K. Singha, S.K. Karmakar, Non-trivial effect of fast vibration on the dynamics of a class of non-linearly damped mechanical systems, *Journal of Sound and Vibration* 260 (4) (2003) 711–730.

[7] M.H. Hansen, Effect of high-frequency excitation on natural frequencies of spinning discs, *Journal of Sound and Vibration* 234 (4) (2000) 577–589.

[8] I.I. Blekhman, *Vibrational Mechanics-Nonlinear Dynamics Effects, General Approach, Applications*, World Scientific, Singapore, 2000.
[9] J.J. Thomsen, Vibration-induced displacement using high-frequency resonators and friction layers, *Kluwer Series: Solid Mechanics and its Applications*, Vol. 37, Kluwer Academic Publishers, Dordrecht, 2000, pp. 237–246.
[10] S. Uhea, Y. Tomikawa, *Ultrasonic Motors, Theory and Applications*, Clarendon Press, Oxford, 1993.
[11] C.C. Canudas de Wit, H. Olsson, K.J. Astrom, P. Lischinsky, A new model for control of systems with friction, *IEEE Transactions on Automatic Control* 40 (3) (1995) 419–425.
[12] P. Dupont, V. Hayward, B. Armstrong, F. Alpeter, Single state elasto-plastic friction models, *IEEE Transactions on Automatic Control* 47 (5) (2002) 787–792.
[13] D.A. Haessig, B. Friedland, On the modeling and simulation of friction, *Journal of Dynamic Systems, Measurement, and Control* 32 (3) (1991) 167–196.
[14] S. Chatterjee, T.K. Singha, S.K. Karmakar, Effect of high-frequency excitation on a class of mechanical systems with dynamic friction, *Journal of Sound and Vibration* 269 (1–2) (2004) 61–89.
[15] A. Isidori, *Nonlinear Control Systems, an Introduction*, Springer, Berlin, 1989.